

The corresponding result in the Glauber theory is obtained by integrating the  $\delta$ -function part of (A3) over a plane tangent at  $(\mathbf{q}+\mathbf{q}')/2$  to a sphere of radius  $q$ . The result is a set of functions  $G_{ij}$  similar to the  $F_{ij}$ .  $G_{00}$  is obtained from  $F_{00}$ , for example, by setting

$$\begin{aligned} \sinh(2yx) &= \sinh(2|q+q'|qR^2) \\ &= \sinh[4q^2R^2 - \Delta q^2R^2/(1+\cos\theta/2)] \\ &\approx \frac{1}{2} \exp[4q^2R^2 - \frac{1}{2}\Delta q^2R^2], \end{aligned}$$

and

$$z/x = qR/|q+q'|R \approx \frac{1}{2}.$$

This is clearly a good approximation for  $qR \gg 1$  and  $(1+\cos\theta/2) \approx 2$ ; however, if we plot  $F_{00}$  and  $G_{00}$  for  $qR \sim 1$ , we find that  $F_{00}$  and  $G_{00}$  differ by 15% or less for all angles.  $F_{01}$  and  $G_{01}$  differ a bit more; the other terms, which are less important, have not been compared explicitly.

Evaluation of triple scattering terms in the Watson

expansion is difficult for this model. However, if  $t_e$  has a radius parameter  $R$ ,  $t_e a^{-1} t_e$  has  $R/\sqrt{2}$ . Thus,  $t_e a^{-1} (t_e a^{-1} t_e)$  is qualitatively similar to the above integrals but with one radius reduced. Hence the triple scattering and higher Glauber terms are useful only as rough estimates; for  $\theta \gtrsim \theta_0$ , where they are relatively important, our calculation is not reliable.

The off-shell scattering, which is omitted in our calculation, is given by the integrals in Eq. (A6). We have evaluated the off-shell parts of  $K_{00}$ ,  $K_{01}$ , and  $K_{11}$  numerically. If the integrals are split into  $y < z$  and  $y > z$  parts, we find that the two are comparable in magnitude and opposite in sign. If the  $c_i$  in Eq. (A1) are given a  $(q''/q)^n$  dependence and included in the integrals, they change greatly. Typically the off-shell amplitudes for model  $A$  are 10 or 20% of the corresponding on-the-energy-shell scattering amplitudes for small  $\theta$ , but are often of the same order or larger for  $\theta \gtrsim \theta_0$ . The off-shell amplitudes for model  $B$  are somewhat larger.

## Nuclear Structure Studies in the Molybdenum Isotopes with $(d,p)$ and $(d,t)$ Reactions\*

SVEN A. HJORTH† AND BERNARD L. COHEN

*University of Pittsburgh, Pittsburgh, Pennsylvania*

(Received 14 April 1964)

Many new energy levels are located in the odd- $A$  molybdenum isotopes and spin and parity values are assigned. In particular, it is found that the ground-state spins of  $\text{Mo}^{99}$  and  $\text{Mo}^{101}$  are both  $\frac{1}{2}^+$ . Occupancy numbers and relative single-quasiparticle energies for the  $2d_{5/2}$ ,  $3s_{1/2}$ ,  $1g_{7/2}$ , and  $2d_{3/2}$  single-quasiparticle states are obtained. The single-quasiparticle energies for  $\text{Mo}^{99}$ , which are equal to the single-particle energies because  $\text{Mo}^{92}$  forms a closed shell, differ only little from those in the isotone  $\text{Zr}^{91}$ . In spite of this, the quasiparticle energies are much lower and the mixing much stronger in the more neutron-rich molybdenum isotopes than in the corresponding zirconium isotopes. A pairing-force calculation revealed that the comparatively small shift in the single-particle levels between zirconium and molybdenum could not account for this completely different behavior of molybdenum and zirconium.

### I. INTRODUCTION

**D**URING the last few years, many nuclear properties have been successfully described by means of the superconductivity model, or pairing theory.<sup>1-3</sup> For instance, the model accounts for the odd-even mass difference, the energy gap in even-even nuclei, and nuclear transition probabilities. With some refinements

it is also possible to calculate the energy of the first excited  $2^+$  and  $3^-$  states as well as their enhanced transition rates with good accuracy.<sup>4,5</sup> The calculations are based upon a knowledge of the unperturbed energy levels of the average shell-model field. Due to meager experimental information, most calculations have, until now, been based upon theoretical estimates of the position of the single-particle levels. Since the result of the calculations depends very sensitively on the single-particle levels, and since the theoretical estimates do not reproduce the finer details of the single-particle levels very well, experimental information on this point is very valuable. In previous papers from this laboratory, single-particle levels have been located in the zir-

\* Work performed at Sarah Mellon Scaife Radiation Laboratory and supported by the National Science Foundation Grant No. GP-2211.

† On leave from The Nobel Institute of Physics, Stockholm, Sweden.

<sup>1</sup> S. T. Belyaev, Kgl. Danske Videnskab. Selskab, Mat. Fys. Medd. **31**, No. 11 (1959).

<sup>2</sup> L. S. Kisslinger and R. A. Sorensen, Kgl. Danske Videnskab. Selskab, Mat. Fys. Medd. **32**, No. 9 (1960).

<sup>3</sup> A. M. Lane, *Nuclear Theory* (W. A. Benjamin, Inc., New York, 1964).

<sup>4</sup> M. Baranger, Phys. Rev. **120**, 957 (1960).

<sup>5</sup> S. Yoshida, Nucl. Phys. **38**, 380 (1962).

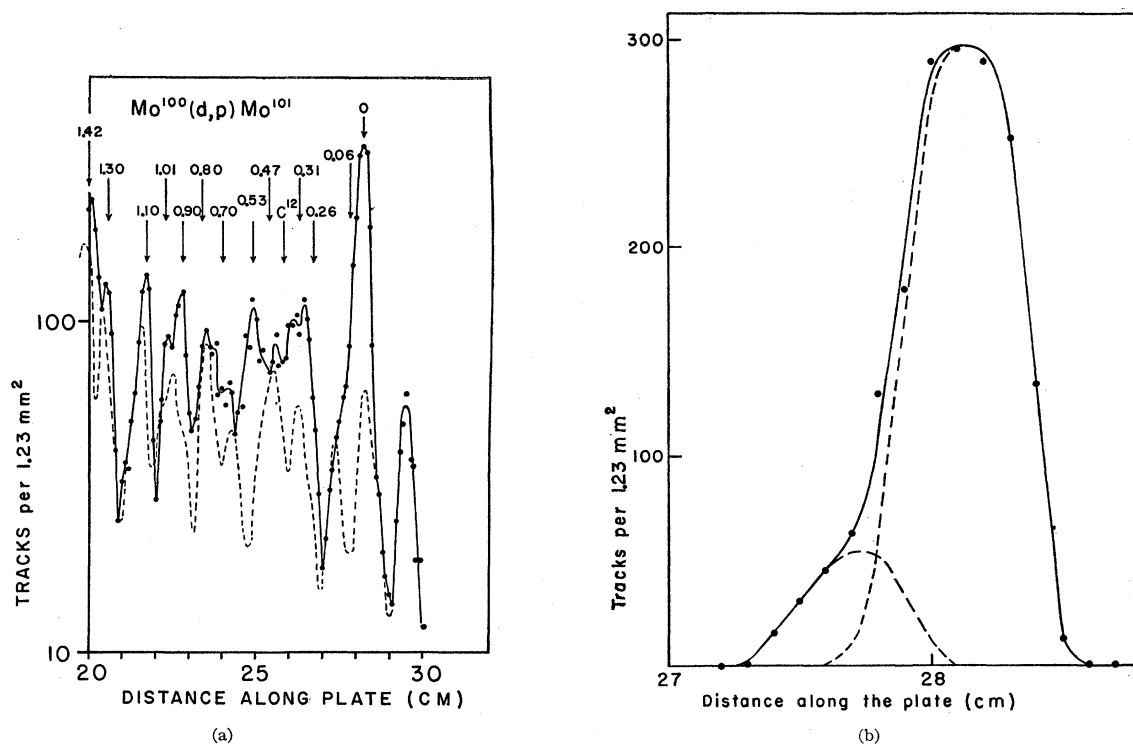


FIG. 1. (a) Energy spectrum of protons from  $\text{Mo}^{100}(d,p)\text{Mo}^{101}$  at  $\theta_{\text{lab}}=9^\circ$ . The dashed lines corresponds to the copper background. (b) The part of the energy spectrum of protons from  $\text{Mo}^{100}(d,p)\text{Mo}^{101}$  at  $\theta_{\text{lab}}=9^\circ$ , which includes the ground-state doublet. The copper background has been subtracted.

conium,<sup>6,7</sup> palladium,<sup>8</sup> tin,<sup>9</sup> barium, and cerium<sup>10</sup> isotopes by  $(d,p)$  and  $(d,t)$  reactions. The procedure of obtaining the single-particle energies from  $(d,p)$  and  $(d,t)$  reactions has been discussed by Yoshida.<sup>5</sup> In these studies it was shown that the single-particle energies do not always show a regular dependence on mass number. This effect was explained by Talmi and by Cohen as due to the long-range neutron-proton interaction. For instance, due to interaction with the  $1g_{7/2}$  protons, the  $1g_{7/2}$  neutron level, which, in zirconium, lies 2.7 MeV above the  $2d_{5/2}$  level, falls below the  $2d_{5/2}$  level in palladium. Also, the  $2d_{3/2}$  and  $1h_{11/2}$  levels appear at lower excitation in palladium than in zirconium. As a consequence, the energy spectra looked completely different. In zirconium the first excited state appears at about 1 MeV, whereas in palladium it is usually within 200 keV from the ground state. Another difference is that the first excited  $2^+$  state lies lower and is more collective in palladium than in zirconium. Molybdenum and ruthenium fall between zirconium and palladium in the periodic table, and the

properties of their  $2^+$  states are also intermediate. In  $\text{Mo}^{92}\text{--}\text{Mo}^{98}$  the energies and transition probabilities of the first excited  $2^+$  state are very close to those in zirconium, but in  $\text{Mo}^{100}$  there is a very abrupt change in energy and transition probability.<sup>11,12</sup> It thus seems very desirable to investigate the single-particle structure of both molybdenum and ruthenium isotopes in order to bridge the gap between zirconium and palladium. Therefore, when enriched targets in the even molybdenum isotopes became available, the following investigation was undertaken.

## II. EXPERIMENTS AND PROCEDURE

Targets enriched to about 90% in the even molybdenum isotopes and a natural molybdenum target were bombarded with 15-MeV deuterons from the University of Pittsburgh Cyclotron. The reaction products were energy analyzed by a  $60^\circ$  magnetic wedge spectrograph and were detected by photographic plates. The details of the experimental system have been described elsewhere.<sup>13</sup> The enriched targets were a mixture of 40%

<sup>6</sup> B. L. Cohen, Phys. Rev. **125**, 1358 (1962).

<sup>7</sup> B. L. Cohen and O. V. Chubinsky, Phys. Rev. **131**, 2184 (1963).

<sup>8</sup> B. Cujec, Phys. Rev. **131**, 735 (1963).

<sup>9</sup> B. L. Cohen and R. E. Price, Phys. Rev. **121**, 176 (1961).

<sup>10</sup> R. H. Fulmer, A. L. McCarthy, and B. L. Cohen, Phys. Rev. **128**, 1302 (1962).

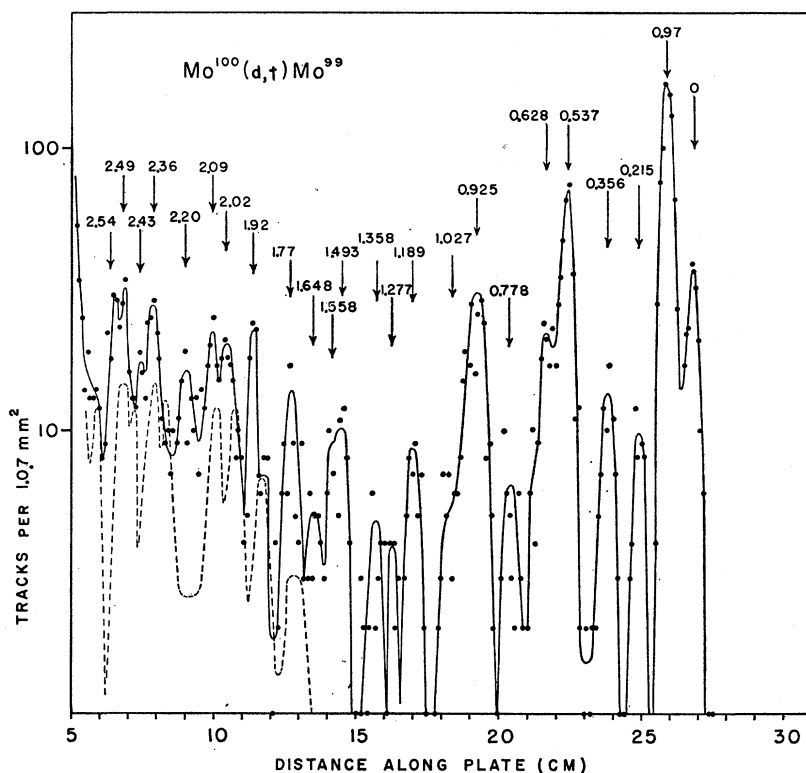
<sup>11</sup> P. H. Stelson and F. K. McGowan, Phys. Rev. **110**, 489 (1958).

<sup>12</sup> G. M. Temmer and N. P. Heydenburg, Phys. Rev. **98**, 1308 (1955).

<sup>13</sup> B. L. Cohen, R. H. Fulmer, and A. L. McCarthy, Phys. Rev. **126**, 698 (1962).

TABLE I. Levels in Mo<sup>98</sup> from Nuclear Data Sheets and from (d,p) and (d,t) reactions.

NDS		(d, p)					(d, t)			
Energy	<i>j</i> π	Energy	<i>l</i>	<i>j</i> π	<i>d</i> σ/ <i>d</i> Ω <sub>max</sub> (mb/sr)	<i>S</i> <sub>d<p></p></sub>	Energy	<i>d</i> σ/ <i>d</i> Ω <sub>45°</sub> (mb/sr)	<i>S</i> <sub>d<i>t</i></sub>	(2 <i>j</i> +1) <i>S</i> <sub>d<p></p></sub> / <i>S</i> <sub>d<i>t</i></sub>
0	(5/2 <sup>+</sup> )		2	$\frac{5}{2}^+$	9.10	0.87	0	1.16	2.29	2.28
0.91		0.944	0	$\frac{1}{2}^+$	3.40	0.70				
1.35										
1.479	(9/2 <sup>+</sup> )									
		1.486	2	$\frac{3}{2}^+$	4.02	0.43				
		1.695	2	$\frac{5}{2}^+$	0.95	0.074				
2.0										
2.16	(13/2 <sup>+</sup> )									
		2.186	(2)	$\frac{3}{2}^+$	0.80	0.083				
		2.300	4	$\frac{7}{2}^+$	0.70	0.37				
2.43	(21/2 <sup>+</sup> )									
		2.445	0	$\frac{1}{2}^+$	0.90	0.15				
		2.700	0	$\frac{1}{2}^+$	1.80	0.30				
2.73	( $\frac{3}{2}^-$ , $\frac{5}{2}^-$ )									
		2.850	2	$\frac{3}{2}^+$	0.90	0.087				
		3.155	2	$\frac{5}{2}^+$	1.77	0.15				
		3.426	2	$\frac{5}{2}^+$	1.55	0.13				
		3.586	2	$\frac{5}{2}^+$	1.30	0.10				
		3.693	2	$\frac{5}{2}^+$	1.05	0.083				

FIG. 2. Energy spectrum of tritons from Mo<sup>100</sup>(d,t)Mo<sup>99</sup> at  $\theta_{lab} = 45^\circ$ . The dashed line corresponds to the copper background.

Mo and 60% Cu and they were rolled to a thickness of 2–3 mg/cm<sup>2</sup>. This limits the resolution to about 50 keV.<sup>14</sup> The natural target was 14.6 mg/cm<sup>2</sup> thick, and it was used to measure the transitions to the ground and first excited states in Mo<sup>95</sup>(d,p)Mo<sup>96</sup> and the ground-state transitions in Mo<sup>92</sup>(d,p)Mo<sup>93</sup> and Mo<sup>97</sup>-(d,p)Mo<sup>98</sup>. All target thicknesses were checked with an

<sup>14</sup> B. L. Cohen, Rev. Sci. Instr. 30, 415 (1959).

alpha-particle thickness gauge. The thicknesses obtained agreed within 10% with those obtained by weighing for the Mo<sup>92</sup>, Mo<sup>98</sup>, and Mo<sup>100</sup> targets. The Mo<sup>94</sup> and Mo<sup>96</sup> targets were found to be very non-uniform and no exact comparison could be made. For all targets except Mo<sup>98</sup> the intensity of the copper background was consistent within 10% with the assumption that 60% of the target thickness was

TABLE II. Levels in Mo<sup>96</sup> from Nuclear Data Sheets and from (d,p) and (d,t) reactions.

NDS		(d,p)					(d,t)			
E	jπ	E	l	jπ	dσ/dΩ <sub>max</sub> mb/sr	S <sub>dp</sub>	E	dσ/dΩ <sub>45°</sub> mb/sr	S <sub>dt</sub>	(2j+1)S <sub>dt</sub> /S <sub>dt</sub>
0	5/2+	0	2	5/2+	8.36	0.74	0	2.04	3.90	1.14
0.204	(5/2+)									
0.752										
0.763										
0.768	(7/2, 3/2+)									
0.784										
0.788	(1/2+, 3/2+)	0.806*	2	3/2+	3.84	0.32	0.79*	0.230	0.250	5.11
0.822		0.806*	0	1/2+			0.87*			
0.932										
1.042	(1/2+, 3/2+)	0.970	2	5/2+	0.45	0.029	0.99	0.193	0.434	0.40
1.071	(5/2+, 3/2+)	1.055	0	1/2+	1.00	0.17	1.09	0.174	0.200	1.70
		1.277	(0)	1+	0.20	0.03	1.20	0.097	0.113	0.53
		1.390	2	3/2+	0.80	0.049	1.44	0.088	0.216	1.36
		(1.478)	?	...	0.53					
		1.630	2	5/2+	1.95	0.11	1.63	0.157	0.394	1.68
		1.80*	(2)	3/2+	0.57	0.042				
		1.80*	(0)	1+			0.025			
		1.95*	(2)	3/2+	0.87	0.046				
		1.95*	(4)	5/2+			0.44			
		2.08*	(0)	1+	3.12	0.25				
		2.08*	(2)	3/2+			0.045			
		2.172	2	5/2+	1.87	0.14				
		2.275	(2)	3/2+	1.15	0.094				
		2.39	(1)	3/2-	2.48	0.098				
		2.52	(0) (1)	1+	0.38	0.095				
		2.62	(2) (1)	3/2-	1.84	0.12				
		2.706	(2)	3/2+	1.12	0.082				
		2.846	2	5/2+	0.74	0.058				
		2.954	0	1+	0.71	0.17				
		3.065	2	3/2+	1.55	0.11				
		3.150*	(4)	5/2+	1.03	0.045				
		3.150*	(1) (2)	3/2-			0.027			

copper. For the Mo<sup>98</sup> target the intensity of the copper background was 25% less than expected.

The proton spectra were recorded at 9°, 16°, 20°, 30°, 38°, and 45°. At all angles background runs on a natural copper target were performed. A typical proton spectrum for Mo<sup>100</sup> is shown in Fig. 1. The relative cross sections at the six angles were compared with distorted-wave Born approximation (DWBA) calculations which had been performed using an Oak Ridge code written by Satchler and collaborators.<sup>15-17</sup> In a previous work on zirconium, where complete angular distributions had been taken, it was found that these calculations fitted the observed cross sections very

<sup>15</sup> The authors are grateful to R. M. Drisko for performing these calculations. Optical model parameters used were

Deuterons:  
 $V = 53.4, r_0 = 1.3, a = 0.79,$   
 $W' = 58.4, r_0' = 1.37, a' = 0.67, r_{0c} = 1.3,$

Protons:  
 $V = 47.43 + (22.2 - E_p)0.55, r_0 = 1.25, a = 0.65,$   
 $W' = 52.4, r_0' = 1.24, a' = 0.65,$   
 $r_{0c} = 1.25, V_s = 8.5.$

Surface derivative absorption, lower cutoff at 6.0 F. (The last makes little difference except for l=0.) The potentials have been obtained from Refs. 16 and 17.

<sup>16</sup> C. M. Perey and F. G. Perey, Phys. Rev. 132, 755 (1963).

<sup>17</sup> F. G. Perey, Phys. Rev. 131, 745 (1963).

well. From our measurement at six angles it was possible to distinguish clearly between l=0, 1, 2 and higher l values, except in cases where the statistics were very bad or the levels not fully resolved. On the other hand, it was usually very difficult to distinguish

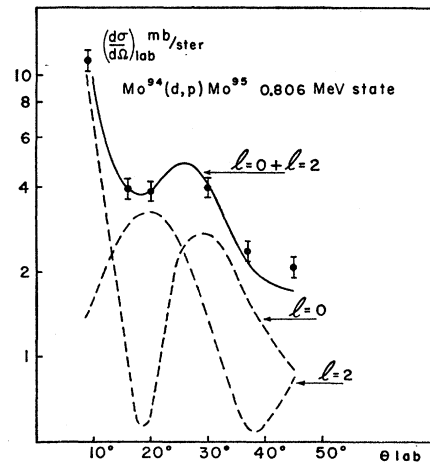


Fig. 3. Angular distribution of protons leading to the 0.806-MeV state in Mo<sup>96</sup>(d,p)Mo<sup>96</sup>. The solid curve is the result of a least-squares fit of l=0 and l=2 DWBA curves to the experimental points. The individual components are shown as dashed lines.

$l=4$  from  $l=3$  and  $l=5$ . Since the shell model does not predict low-lying  $l=3$  transitions in this region, and since no  $l=5$  transitions had been observed in zirconium, all transition which were compatible with  $l=4$  were given that assignment. In some cases the data could not be fitted with a single  $l$ -DWBA curve, and in those cases a mixture that gave good agreement with data was assumed. Spectroscopic factors were obtained by comparing the absolute cross sections with the DWBA calculations. The calculations should be reliable to within about 50%. In fact, the excellent

agreement with shell-model predictions in the zirconium case seems to indicate that the calculations are much better than that. The error in the absolute cross sections due to error in geometry, plate reading, current integration, and target thickness is about 20%. For the weaker groups, poor statistics due to the copper background limits the accuracy in the absolute cross section to very roughly  $\pm 0.15$  mb. This also approximately constitutes the upper limit to states not observed in this study. In cases of unresolved doublets, an additional large error is introduced in  $S$  due to the

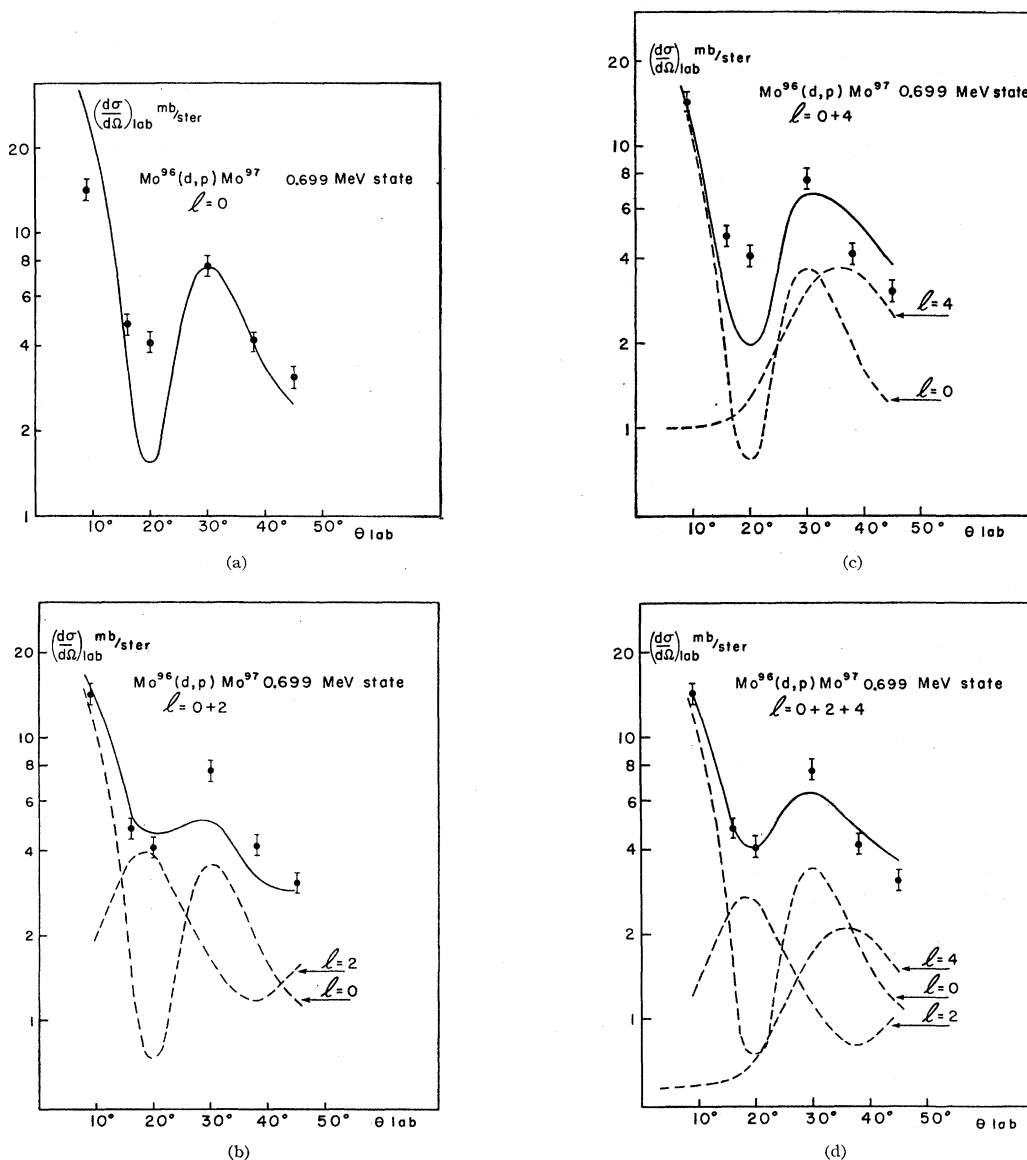


FIG. 4. Fits to the experimental angular distribution of protons from  $\text{Mo}^{96}(d,p)\text{Mo}^{97}$ , 0.699-MeV state. (a) The solid curve is the experimental angular distribution of protons from  $\text{Mo}^{96}(d,p)\text{Mo}^{97}$  ground state. (b) A least-squares fit of  $l=0$  [from  $\text{Mo}^{96}(d,p)\text{Mo}^{97}$  ground state] and  $l=2$  [from  $\text{Mo}^{98}(d,p)\text{Mo}^{99}$ , 0.100-MeV state]. The individual components are shown as dashed lines. (c) A least-squares fit of  $l=0$  (from  $\text{Mo}^{96}(d,p)\text{Mo}^{97}$  ground state) and  $l=4$  (from DWBA). The individual components are shown as dashed lines. (d) A least-squares fit of  $l=0$  (from  $\text{Mo}^{96}(d,p)\text{Mo}^{97}$  ground state),  $l=2$  [from  $\text{Mo}^{98}(d,p)\text{Mo}^{99}$ , 0.100-MeV state] and  $l=4$  (from DWBA). The individual components are shown as dashed lines.

TABLE III. Levels in Mo<sup>97</sup> from Nuclear Data Sheets and from (d,p) and (d,t) reactions.

NDS		(d,p)					(d,t)			
E	j <sub>π</sub>	E	l	j <sub>π</sub>	dσ/dΩ <sub>max</sub> mb/sr	S <sub>d<sub>p</sub></sub>	E	dσ/dΩ <sub>45°</sub> mb/sr	S <sub>d<sub>t</sub></sub>	(2j+1)S <sub>d<sub>p</sub></sub> /S <sub>d<sub>t</sub></sub>
0	5/2 <sup>+</sup>	0	2	5/2 <sup>+</sup>	5.23	0.42	0	3.06	5.82	0.43
0.67	(7/2 <sup>+</sup> , 9/2 <sup>+</sup> )	(0.699*)	(4)	7/2 <sup>+</sup>	7.60	1.28	(0.695*)	0.750	0.79	
		0.699*	0	9/2 <sup>+</sup>		0.55	0.695*			
		(0.699*)	(2)	5/2 <sup>+</sup>		0.28	(0.695*)			
1.02		0.893	0	3/2 <sup>+</sup>	0.70	0.11	0.900	0.075	0.082	2.93
		1.271	2	5/2 <sup>+</sup>	3.96	0.34	1.136	0.038		
		1.450*	(2)	7/2 <sup>+</sup>	0.70	0.037	1.288	0.258	0.61	2.23
		1.450*	(4)	9/2 <sup>+</sup>		0.30				
		1.554	3	5/2 <sup>+</sup>	1.44	0.22	1.56	0.047		
		1.70	(2)	7/2 <sup>+</sup>	0.33	0.024	1.71	0.051 <sup>a</sup>	0.25	0.60
		1.78	(4)	9/2 <sup>+</sup>	0.47	0.24	1.78	0.100 <sup>a</sup>	2.04	0.94
		1.96	2	5/2 <sup>+</sup>	0.38	0.030				
		2.065	0	7/2 <sup>+</sup>	0.72	0.15	2.06	0.062	0.059	5.10
		2.153	2	9/2 <sup>+</sup>	2.90	0.22	2.17	0.143	0.248	3.55
		2.35	(1)	5/2 <sup>-</sup>	0.75	0.030				
		2.46	(1)	3/2 <sup>-</sup>	0.91	0.035				

<sup>a</sup> Obtained at 60° because the copper background made it impossible to make the evaluation at 45°.

fitting procedure. The excitation energies could usually be determined with an accuracy of about ±10 keV for the strongly excited states. For weakly excited states the intense copper background made the errors in localizing the peaks greater, so in some cases the excitation energies are not more accurate than to about ±20 keV. In those cases the excitation energies are only given to two figures.

The (d,t) reactions were studied at 45° and 60° for Mo<sup>94</sup>, Mo<sup>96</sup>, Mo<sup>98</sup>, and Mo<sup>100</sup>. A spectrum for Mo<sup>100</sup>-(d,t)Mo<sup>99</sup> is shown in Fig. 2. No runs were made on Mo<sup>92</sup> since the Q value for this reaction is so negative that the tritons are lost in the deuteron background. For the same reason only data for the ground-state transition in Mo<sup>94</sup>(d,t)Mo<sup>93</sup> could be obtained.

The accuracy in the absolute cross sections and excitation energies is limited by the same considerations as in the (d,p) case. For the weakest states the statistics limits the accuracy in absolute cross sections to about 30%. Spectroscopic factors for the (d,t) reactions were obtained by comparing the absolute cross sections at 45° with the corresponding cross sections in Zr<sup>96</sup>, where the relation between cross sections and spectroscopic factors are known.<sup>7</sup> As in Ref. 7, we assumed that the cross sections could be written as

$$\sigma(d,t) = T_l K^Q S(d,t). \quad (1)$$

The values of T<sub>l</sub> and K found empirically are very roughly T<sub>0</sub>=2T<sub>2</sub>=8T<sub>4</sub> and K=1.18. In Zr<sup>96</sup>(d,t)Zr<sup>95</sup>, Q=-1.605, l=2, the absolute cross section at 47° is 3.76 mb and S is 5.75. Neglecting the difference in angle by 2°, we obtain T<sub>0</sub>=1.708, T<sub>2</sub>=0.854, and T<sub>4</sub>=0.213. The spectroscopic factors obtained in this fashion are believed to be accurate to about 40%.

### III. RESULTS

#### A. General

The results from the measurement of the (d,p) and (d,t) reactions leading to the same final nucleus are shown in Tables I-V and in Fig. 6. In the tables are also included what is known about the nuclei from the Nuclear Data Sheets.<sup>18</sup> The cross sections that are listed, dσ/dΩ<sub>max</sub>, are those at the first maximum beyond 9° in the angular distribution, that is, usually 30° for l=0, 9° for l=1, 20° for l=2, 30° for l=3, and

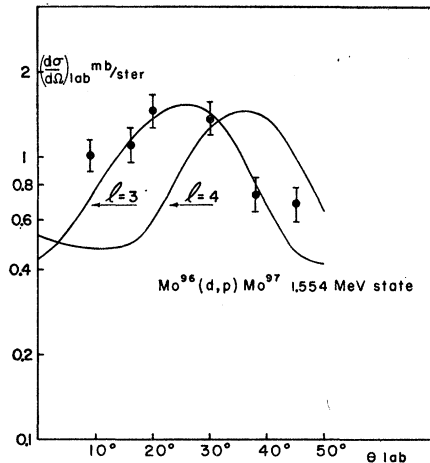


Fig. 5. Assignment of the 1.559-MeV state in Mo<sup>97</sup> by comparing the experimental angular distribution from Mo<sup>96</sup>(d,p)Mo<sup>97</sup> with l=3 and l=4 DWBA curves.

<sup>18</sup> Nuclear Data Sheets, compiled by K. Way et al. (Printing and Publishing Office, National Academy of Sciences—National Research Council, Washington 25, D. C., 1960), NRC 60-05-091, 60-05-120, 60-06-073, 61-01-079, 61-02-026.

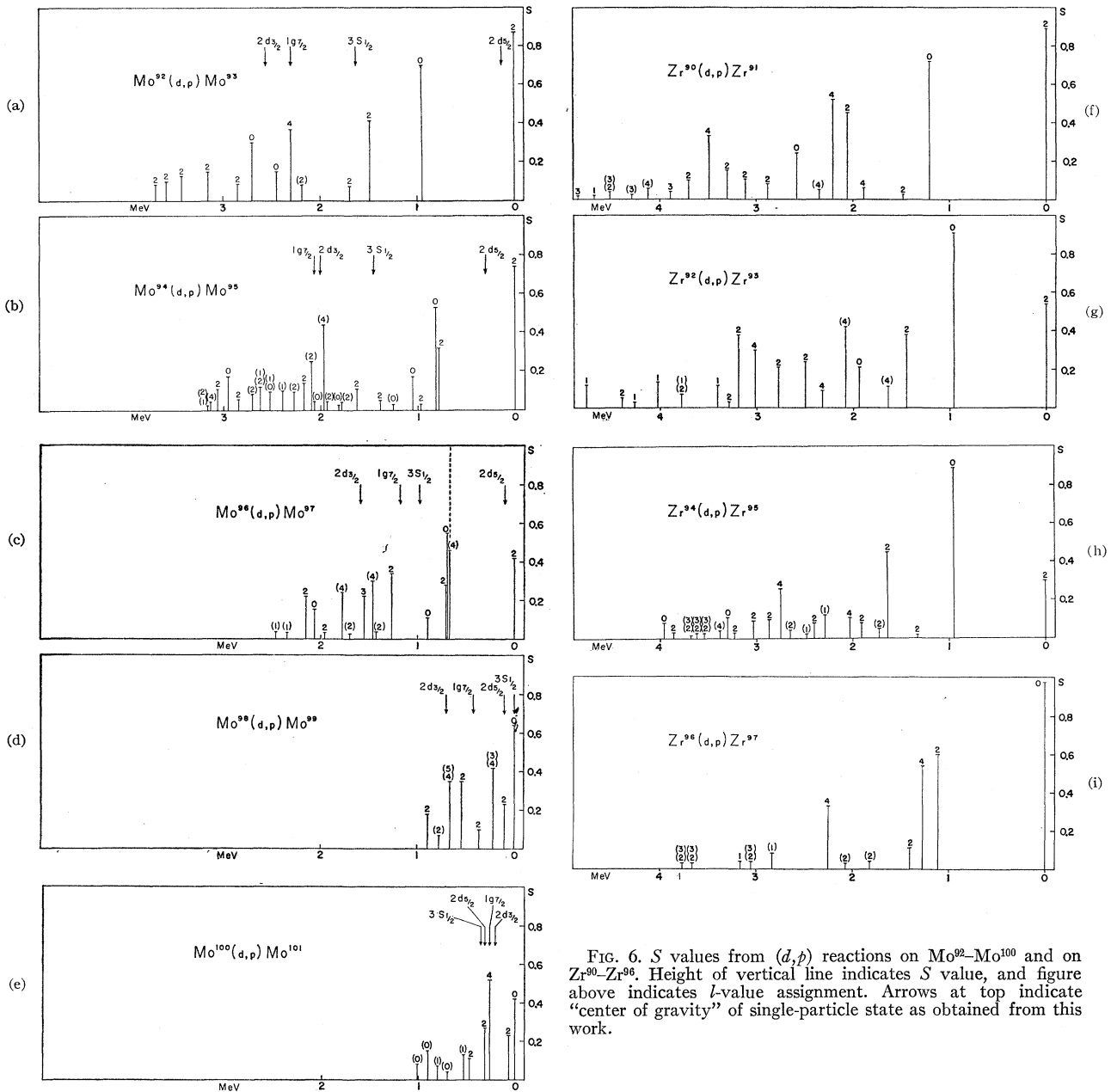


FIG. 6.  $S$  values from  $(d,p)$  reactions on  $\text{Mo}^{92}\text{--}\text{Mo}^{100}$  and on  $\text{Zr}^{90}\text{--}\text{Zr}^{96}$ . Height of vertical line indicates  $S$  value, and figure above indicates  $l$ -value assignment. Arrows at top indicate "center of gravity" of single-particle state as obtained from this work.

30–38° for  $l=4$ . Spin assignments were made with the aid of the predictions of the shell model. An ambiguity arises in the case of  $l=2$ . In this case, however, it is expected that  $(2j+1)S_{dp}/S_{dt}$  should be much larger for  $j=3/2$  than for  $j=5/2$  because the  $2d_{5/2}$  state is lower and therefore more full than the  $2d_{3/2}$  state. The reason for this can be seen from Eqs. (2) and (3) in Sec. IV. The ground states of  $\text{Mo}^{95}$  and  $\text{Mo}^{97}$  are known to be  $5/2^+$ , and in those nuclei states with  $(2j+1)S_{dp}/S_{dt}$  around that of the ground states were assigned  $5/2^+$ , the others  $3/2^+$ . In  $\text{Mo}^{98}$  the ground state is believed to be  $5/2^+$  from  $\gamma\gamma$ -angular correlation and  $\beta$ -decay work and

the value of  $(2j+1)S_{dp}/S_{dt}$  confirms that. In  $\text{Mo}^{99}$  the value of  $(2j+1)S_{dp}/S_{dt}$  is considerably lower for the 0.100-MeV state than for the others, and accordingly, this state is assigned  $5/2^+$  whereas the others are assigned  $3/2^+$ . From Tables IV and V we also note that the proposed ground-state spin of  $\text{Mo}^{99}$   $1/2^+$  is confirmed, and that the ground-state spin of  $\text{Mo}^{101}$  is  $1/2^+$ .

### B. $\text{Mo}^{92}(d,p)\text{Mo}^{93}$

As can be seen from Table I, the assignment of  $l$  values was straightforward and unambiguous in all

TABLE IV. Levels in Mo<sup>98</sup> from Nuclear Data Sheets and from (d,p) and (d,t) reactions.

NDS			(d,p)				(d,t)			
E	j $\pi$	E	l	j $\pi$	d $\sigma$ /d $\Omega_{\max}$ mb/sr	S <sub>dp</sub>	E	d $\sigma$ /d $\Omega_{45^\circ}$ mb/sr	S <sub>dt</sub>	(2j+1)S <sub>dp</sub> /S <sub>dt</sub>
0	( $\frac{1}{2}^+$ )	0	0	$\frac{1}{2}^+$	3.96	0.64	0	0.395	0.33	3.93
0.098		0.100	2	$\frac{3}{2}^+$	3.43	0.23	0.097	1.76	2.98	0.46
0.260		0.222	(3) (4)	$\frac{7}{2}^+$	0.85	0.42	0.215	0.132	0.90	3.73
		0.361	2	$\frac{3}{2}^+$	1.15	0.10	0.356	0.170	0.30	1.34
		0.545	2	$\frac{5}{2}^+$	4.24	0.35	0.537	0.684	1.21	1.16
		0.664	(4) (5)	$\frac{7}{2}^+$	0.70	0.35	0.628	0.318	2.43	1.15
		0.774	(2)	$\frac{5}{2}^+$	0.80	0.070	0.778	0.088	0.17	1.70
		0.899	2	$\frac{7}{2}^+$	2.00	0.18	0.925	0.440	0.85	0.85
							1.027	0.071		
							1.189	0.098		
							1.277	0.028		
							1.358	0.044		
							1.493	0.076		
							1.558	0.075		
							1.648	0.051		
							1.77	0.087		
							1.92	0.113		
							2.02	0.104		
							2.09	0.149		
							2.20	0.163		
							2.36	0.110		
							2.43	0.063		
							2.49			
							2.54	0.260		

TABLE V. Levels in Mo<sup>101</sup> from Nuclear Data Sheets and from (d,p) and (d,t) reactions.

NDS			(d,p)				(d,t)			
E	j $\pi$	E	l	j $\pi$	d $\sigma$ /d $\Omega_{\max}$ mb/sr	S <sub>dp</sub>	E	d $\sigma$ /d $\Omega_{\max}$ mb/sr	S <sub>dt</sub>	(2j+1)S <sub>dp</sub> /S <sub>dt</sub>
0	( $\frac{5}{2}^+$ )	0* } 0.06* } 0.26* } 0.31* } 0.47* } 0.53* } 0.70 } 0.80 } 0.90 } 1.01 } 1.10 } 1.30* } 1.42* }	0 2 4 2 2 (1) (0) (1) (0) (0) (0)	$\frac{1}{2}^+$ $\frac{3}{2}^+$ $\frac{7}{2}^+$ $\frac{5}{2}^+$ $\frac{3}{2}^+$ $\frac{3}{2}^-$ $\frac{1}{2}^+$ $\frac{3}{2}^-$ $\frac{1}{2}^+$ $\frac{1}{2}^+$	2.9 2.5 1.08 4.65 1.19 2.15 0.22 1.36 0.71 0.59 0.65 0.76	0.42 0.23 0.52 0.28 0.11 0.13 0.04 0.07 0.15 0.08				

cases, but one where the statistics was not good enough. Since no (d,t) data are available for the excited states, there is no means to distinguish  $j=\frac{3}{2}^+$  from  $j=\frac{5}{2}^+$ . However, the  $\frac{5}{2}^+$  single-particle state which is lower is not expected to be distributed over a wide energy region, and since the excited  $l=2$  states appear at a fairly high excitation energy we expect them to be  $\frac{3}{2}^+$ . This consideration should also apply to Mo<sup>95</sup>, but there the (d,t) reaction suggests at least one excited  $\frac{5}{2}^+$  state. Also, Ball and Bhatt<sup>19</sup> using the method of effective interaction predict two excited  $\frac{5}{2}^+$  states in Mo<sup>98</sup>. The states appear at 1.54- and 2.99-MeV excitation and should have the stripping spectro-

scopic factors 0.03 and 0.005, respectively. It thus seems reasonable to assume that our 1.69-MeV state is  $\frac{5}{2}^+$  and that all other  $l=2$  transitions go to  $\frac{3}{2}^+$  states.

### C. Mo<sup>94</sup>(d,p)Mo<sup>95</sup>

The result of this reaction is displayed in Table II and Fig. 6. We observe that the level density in Mo<sup>95</sup> seems to be much higher than in the neighboring molybdenum isotopes. This may be due to the fact that the Mo<sup>94</sup> target was only enriched to about 80% in Mo<sup>94</sup>. In fact, it contained as much as 9.6% Mo<sup>95</sup>. It thus seems quite possible that some of the levels listed in Table II really belong to Mo<sup>96</sup> (and maybe other molybdenum isotopes), but since we did not have a Mo<sup>95</sup> target there was no means to check upon that.

<sup>19</sup> J. B. Ball and K. H. Bhatt, Bull. Am. Phys. Soc. **9**, 483 (1964).



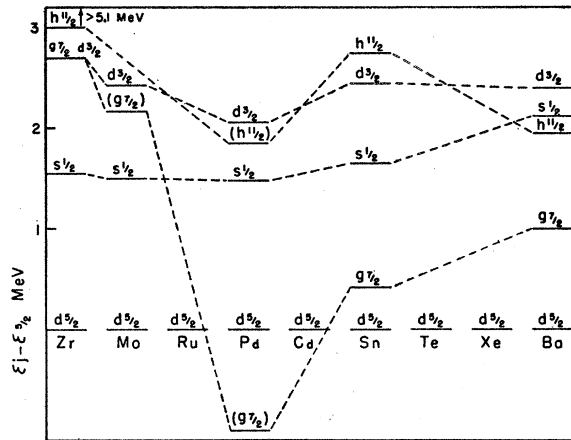


FIG. 7. Relative single-particle energy levels as determined by stripping and pickup reactions in nuclei within the 50-82 neutron shell.

Due to the high-level density in the spectrum, many levels were unresolved and a mixture of different  $l$  values had to be assumed in order to fit the angular distributions. The most important of these cases is the transition to the 806-keV state in  $\text{Mo}^{95}$ . The angular distribution for this transition looks like a  $l=0$  except that the first minimum has disappeared and the point at  $9^\circ$  seems to be too low (Fig. 3). However, an excellent fit was obtained if a mixture of  $l=0$  and  $l=2$  was assumed. That this transition may be a mixture is confirmed by the Nuclear Data Sheets (Table II). In fact, there are no less than 6 close-lying levels with different spins at about this excitation in  $\text{Mo}^{95}$ .

#### D. $\text{Mo}^{96}(d,p)\text{Mo}^{97}$

The result from this reaction is shown in Table III and Fig. 6. As in the case of  $\text{Mo}^{94}(d,p)\text{Mo}^{95}$  the angular distribution of protons leading to the 699-keV state seems to be complicated. This is shown in Fig. 4, where the measured angular distribution is compared with the ground-state transition in  $\text{Mo}^{98}(d,p)\text{Mo}^{99}$ . These reactions have about the same  $Q$  and the latter reaction should therefore have almost the same angular distribution as a pure  $l=0$  transition to the 699-keV state in  $\text{Mo}^{96}(d,p)\text{Mo}^{97}$ . The fit is obviously not very good, and furthermore, the spectroscopic factor extracted from this fit makes the  $\sum_n S_{1/2}^{(n)}(d,p)$  60% larger than its theoretical upper limit (see Sec. IV). This is larger than the error in our measurements and extraction procedure, which are definitely smaller than 50%. It is true that we can obtain a better fit by saying that there is an error of about  $3^\circ$  in the angle, but then there still remains to be explained the abnormally large cross section and a fit which by no means is perfect. We therefore try, as in  $\text{Mo}^{94}(d,p)\text{Mo}^{95}$ , to fit the angular distribution with an  $l=0+l=2$  transition. A least-square fit shown in Fig. 4(b) does not look very convincing.

If we observe that the Nuclear Data Sheets suggests a  $j=\frac{7}{2}^+$  level at 0.67-MeV excitation, and if we assume that this level is excited, we obtain the fit shown in Fig. 4(c). The fit is again not very good, and furthermore, the spectroscopic factor for the  $l=4$  transition becomes almost three times as large as its theoretical upper limit. Finally, we try to fit the transition with a sum of  $l=0$  and  $l=2+l=4$  transitions [Fig. 4(d)]. The spectroscopic factor for the  $l=4$  transition is still a little too large, but this is not too disturbing since the error in the fitting procedure is very large. Also, the  $l=4$  spectroscopic factor is very sensitive to the angle. A slight error in angle may easily change the  $l=4$  spectroscopic factor by a factor of two and leave the other two essentially unchanged. Since the fit to the angular distribution is by far the best in this case, we assume that this transition really goes to a triplet of states. This assumption is further strengthened by the fact that the sum rule for  $l=2$ ,  $j=\frac{3}{2}$ ,  $(d,p)$  and  $(d,t)$  transitions from the target nucleus  $\text{Mo}^{96}$  is not very well exhausted. If the missing strength should be present at higher excitation, it would move the  $\frac{3}{2}^+$  single-particle state to higher excitation. This does not seem very likely as can be seen from Fig. 7. In this reaction there is also a remarkably strong  $l=3$  transition, the analog of which has not been observed in the other molybdenum isotopes. The angular distribution of this transition is shown in Fig. 5. Clearly, it is excellently fitted, with a  $l=3$  DWBA curve, whereas a  $l=4$  curve gives a very poor fit indeed.

#### E. $\text{Mo}^{93}(d,p)\text{Mo}^{99}$

The result of this reaction is displayed in Table IV and Fig. 6. Due to the intense copper background and possible carbon impurities, it was impossible to analyze transitions to states of higher excitation than 0.900 MeV in  $\text{Mo}^{99}$ . It follows that there does not seem to be any more strongly excited states below 2 MeV in  $\text{Mo}^{99}$ . This is markedly different from the case in the isotone  $\text{Zr}^{97}$ , where the first excited state appears at 1.1 MeV. This difference will be further analyzed in the discussion.

#### F. $\text{Mo}^{100}(d,p)\text{Mo}^{101}$

The result of this reaction is shown in Table V and Fig. 6. In this case, there are no less than three low-

TABLE VI.  $\text{Mo}^{95}(d,p)\text{Mo}^{96}$  and  $\text{Mo}^{97}(d,p)\text{Mo}^{98}$ .

$E$	$l$	$d\sigma/d\Omega_{\text{max}}$ mb/sr	$S$
$\text{Mo}^{95}(d,p)\text{Mo}^{96}$			
0	2	0.61	2.48
0.81	2	0.46	0.30
	0	0.15	0.08
$\text{Mo}^{97}(d,p)\text{Mo}^{98}$			
0	2	0.71	2.50

lying doublets. The energy separation of the members of the doublets, however, was large enough to permit an estimate of their angular distributions from considerations of their peak heights. For instance, that the lowest member of the ground-state doublet is  $\frac{1}{2}^+$  is clearly seen from Fig. 1(b). The peak corresponding to the ground state is much higher. At all other angles the peaks were of comparable height. For the two lowest doublets it was not practical to attempt to separate the peaks, so the spectroscopic factors were obtained by a least square fit to the cross section. Since no  $(d,t)$  reaction leading to  $\text{Mo}^{101}$  could be performed, there was again no means to distinguish  $j=\frac{3}{2}^+$  from  $j=\frac{5}{2}^+$ . For the purpose of the following discussion, we assumed that the state at 0.31 MeV is  $\frac{5}{2}^+$ , and that the two others are  $\frac{3}{2}^+$ .

#### G. $\text{Mo}^{94}(d,t)\text{Mo}^{93}$

In this reaction only the ground-state transition could be observed as can be seen from the results in Table I.

#### H. $\text{Mo}^{96}(d,t)\text{Mo}^{95}$

The tritons leading to the excited states were superimposed on a copper background, and since the statistics were not very good, the result in Table II can only be regarded as tentative. Clearly, the agreement between excitation energies obtained from the  $(d,p)$  and the  $(d,t)$  reactions leaves much to be desired.

#### I. $\text{Mo}^{98}(d,t)\text{Mo}^{97}$

In this reaction the  $Q$  value was sufficiently high so that many levels could be studied without interference with the copper background. The agreement between levels observed in the  $(d,p)$  and the  $(d,t)$  reactions is also satisfactory in this case, as can be seen in Table III.

#### J. $\text{Mo}^{100}(d,t)\text{Mo}^{99}$

The  $Q$  value was still higher in this case and this permitted us to observe levels up to an excitation of 2.5 MeV in  $\text{Mo}^{99}$ . The result from this reaction is thus much better than for the  $(d,p)$  case where we only could observe levels up to 0.9 MeV. We also note that no strongly excited states occur above 0.9-MeV excitation in  $(d,t)$  and thus support our conclusion that no strongly excited states appear in  $(d,p)$  at higher energies.

#### K. $\text{Mo}^{95}(d,p)\text{Mo}^{96}$ and $\text{Mo}^{97}(d,p)\text{Mo}^{98}$

These reactions were performed on a thick natural molybdenum target and only the ground states and the first excited state in  $\text{Mo}^{96}$  could be studied. The results are listed in Table VI.

### IV. SUM RULES, SINGLE-QUASIPARTICLE ENERGIES AND OCCUPANCY NUMBERS

#### A. Sum Rules

The spectroscopic factors  $S_j$  obey sum rules related to the occupancy numbers  $U_j^2$  and  $V_j^2$  of the pairing

theory.<sup>1-3</sup> According to Yoshida<sup>5</sup> we have for an even-even target nucleus

$$\sum_n (2j+1)S_j^{(n)}(d,p) = (2j+1) \left[ U_j^2 + \frac{2\lambda+1}{2j+1} \times \sum_{j'} (\varphi^{jj'a\lambda})^2 V_j'^2 \right], \quad (2)$$

$$\sum_m S_j^{(m)}(d,t) = (2j+1) \left[ V_j^2 + \frac{2\lambda+1}{2j+1} \times \sum_{j'} (\varphi^{jj'a\lambda})^2 U_j'^2 \right], \quad (3)$$

where  $n$  and  $m$  label individual nuclear states with a given  $j$ .

$U_j^2$  is the extent to which the single-particle neutron level  $j$  is empty and  $V_j^2$  is the extent to which the single-particle neutron level  $j$  is occupied in the even-even target nucleus. The  $\varphi$ 's are the amplitudes of the three-quasiparticle excitation. They are usually small and, according to Yoshida, the second term is normally only a few percent of the first and may therefore be neglected. Obviously  $U_j^2$  and  $V_j^2$  obey the following relation:

$$U_j^2 + V_j^2 = 1. \quad (4)$$

Neglecting the  $\varphi$ 's we obtain from (2), (3), and (4)

$$\sum_n (2j+1)S_j^{(n)}(d,p) + \sum_m S_j^{(m)}(d,t) \approx 2j+1, \quad (5)$$

where  $S_j^{(n)}(d,p)$  and  $S_j^{(m)}(d,t)$  refer to the same target nucleus and consequently to different final nuclei. We also note that

$$\sum_j \sum_n (2j+1)S_j^{(n)}(d,p) \approx \text{number of neutron holes in the nuclear cloud of the even-even nucleus} \quad (6)$$

and

$$\sum_j \sum_m S_j^{(m)}(d,t) \approx \text{number of neutrons in the nuclear cloud of the even-even nucleus.} \quad (7)$$

Obviously

$$\begin{aligned} \sum_j \sum_n (2j+1)S_j^{(n)}(d,p) + \sum_j \sum_m S_j^{(m)}(d,t) \\ \approx \sum_j (2j+1) = \text{number of available neutron states.} \end{aligned} \quad (8)$$

These sums are computed and compared with their theoretical values in Table VII. The root-mean-square error of  $\sum_n (2j+1)S_j^{(n)}(d,p) + \sum_m S_j^{(m)}(d,t)$  is about 16% if the  $g_{7/2}$  transitions for which the data are very poor, are excluded. In view of the approximate nature of the formula used, the errors in the spectroscopic factors, the fact that not all levels have been observed and that some weakly excited levels may be improperly assigned, the agreement must be said to be satisfactory. It also gives confidence that the most important levels are correctly accounted for. Some features of Table VII

TABLE VII.  $\sum_n (2j+1)S_j^{(n)}(d,p)$ ,  $\sum_m S_j^{(m)}(d,t)$ , and  $\sum_n (2j+1)S_j^{(n)}(d,p) + \sum_m S_j^{(m)}(d,t)$  for  $(d,p)$  and  $(d,t)$  reactions on the given target nucleus.

	Mo <sup>92</sup>		Mo <sup>94</sup>		Mo <sup>96</sup>		Mo <sup>98</sup>		Mo <sup>100</sup>		Theory				
	(d, p)	(d, t)	(d, p)	(d, t)	(d, p)	(d, t)	(d, p)	(d, t)	(d, p)	(d, t)					
2d <sub>5/2</sub>	5.64		5.58	2.29	7.87	2.64	4.33	6.97	1.38	6.07	7.45	1.62	2.98	4.60	6
3s <sub>1/2</sub>	2.30		2.14			1.62	0.52	2.14	1.28	0.93	2.21	1.38	0.33	1.71	2
2d <sub>3/2</sub>	4.24		4.56			3.62	0.25	3.87	2.80	0.86	3.66	1.36	2.52	3.88	4
1g <sub>7/2</sub>	2.96		3.88			4.30		4.30	6.15	>2.04	8.19	4.16	3.30	7.46	8
						14.50		14.50							
Σ	15.14		16.16	2.29		12.18– 22.98	5.10	17.28– 27.48	11.61	>9.90	21.51	8.52	9.13	17.65	
Theory	20	0	20	18	2	20	16	4	20	14	6	20	12	8	20

need additional discussion. We note that the main part of the discrepancy in Table VII comes from the  $\frac{5}{2}^+$  transitions. It seems as if the spectroscopic factors are overestimated in this case. If the data had been compared with DWBA calculations for Zr, in which a deeper deuteron potential had been used,<sup>7</sup> all the  $(d,p)$  spectroscopic factors would have come out about 30% smaller. The discrepancy in this case would have been of opposite sign and slightly larger, and furthermore, the spectroscopic factor for Mo<sup>92</sup>(d,p)Mo<sup>93</sup> g.s. turns out to be only 0.73. For this case we expect  $S \approx 1$  because Mo<sup>92</sup> has a closed neutron shell structure and it would be hard to explain a  $S$  as small as 0.7. Also, this reaction was studied with the natural target and the error in the absolute cross section is small, probably less than 10%. Although the evidence is not conclusive, it seems as if the shallow deuteron potential ( $V \approx 50$  MeV)<sup>15,16</sup> works better than the deeper ( $V \approx 70$  MeV).<sup>7</sup> This is in contradiction to the general belief that deuteron potentials should be 70–100 MeV deep.<sup>20,21</sup>

We further note from Table VII that we have missed a considerable fraction of the  $g_{7/2}$  strength in Mo<sup>92</sup> and Mo<sup>94</sup>, and probably also part of the  $d_{3/2}$  strength in Mo<sup>96</sup> and Mo<sup>94</sup>. In Mo<sup>100</sup> we note that the  $(d,t)$  transitions to  $\frac{3}{2}^+$  levels in Mo<sup>99</sup> are surprisingly strong and that transitions to  $\frac{5}{2}^+$  states are surprisingly weak. This feature is very persistent and does not change unless one assumes that more levels in Mo<sup>99</sup> are  $\frac{5}{2}^+$  instead of  $\frac{3}{2}^+$ . In view of the sum rule for Mo<sup>98</sup> (Table VII), however, this does not seem very probable.

## B. Single-Quasiparticle Energies

The single-quasiparticle energies  $E_j$ , relative to the  $E_{5/2}$  single-quasiparticle energy are taken as

$$E_j - E_{5/2} = \frac{\sum_n S_j^{(n)}(d,p)E_j^{(n)}}{\sum_n S_j^{(n)}(d,p)} - \frac{\sum_n S_{5/2}^{(n)}(d,p)E_{5/2}^{(n)}}{\sum_n S_{5/2}^{(n)}(d,p)}. \quad (9)$$

<sup>20</sup> G. R. Satchler, in Proceedings of the Symposium on Nuclear Spectroscopy with Direct Interactions, Chicago, 1964 (unpublished).

<sup>21</sup> L. L. Green, in Proceedings of the Symposium on Nuclear Spectroscopy with Direct Interactions, Chicago, 1964 (unpublished).

For  $j = \frac{3}{2}^+$  transitions in Mo<sup>96</sup>(d,p)Mo<sup>97</sup>, the sum rule (5) was not very well fulfilled and the missing strength was assumed to be present at the highest level observed. The same was true for Mo<sup>98</sup>(d,p)Mo<sup>99</sup>  $j = \frac{3}{2}^+$ , but here the good  $(d,t)$  data suggested a better correction method. We assumed that  $(2j+1) \cdot S_j^{(n)}(d,p) = S_j^{(n)}(d,t)$ , which is suggested by Table VII. We further assumed that the lowest levels in Mo<sup>99</sup> above 0.90 MeV are all  $\frac{3}{2}^+$ , and that there are as many  $\frac{3}{2}^+$  states as the sum rule requires.

Obviously the data for the  $g_{7/2}$  shell are very poor. Not only do we miss most of the strength in Mo<sup>92</sup>(d,p)Mo<sup>93</sup> and Mo<sup>94</sup>(d,p)Mo<sup>95</sup>, but also, all  $l=4$  transitions are more or less uncertain. In Mo<sup>96</sup> the  $l=4$  transition to the first excited state is much more poorly determined than the others, and for the purpose of this analysis we assumed that it is only excited insofar as the sum rule (5) is fulfilled. The single-quasiparticle energies obtained in this fashion for the odd-molybdenum isotopes are listed in Table VIII. We also computed the single-quasiparticle energies from the spectroscopic factors obtained from the other DWBA calculation,<sup>7</sup> and consequently, different assumptions on the missing strength. The energies obtained in this fashion usually fell within 200 keV from the values listed in Table VIII, and thus suggest that the single-quasiparticle energies as obtained from (9) are accurate to within that amount.

From considerations of three-quasiparticle excitation using the random-phase approximation (RPA) method, Yoshida<sup>5</sup> finds that the following formula gives a better

TABLE VIII. Single-quasiparticle energies for neutrons relative to the  $\frac{5}{2}^+$  single-quasiparticle energy in the molybdenum isotopes obtained from  $(d,p)$  reactions in the case of odd isotopes,  $(d,p)$ , and  $(d,t)$  reactions in the case of even isotopes.

State	Mo <sup>93</sup>	Mo <sup>95</sup>	Mo <sup>97</sup>	Mo <sup>98</sup>	Mo <sup>99</sup>	Mo <sup>100</sup>	Mo <sup>101</sup>
3s <sub>1/2</sub>	1.50	1.15	0.88	0.69	-0.10	0.09	0.04
1g <sub>7/2</sub>	(2.17)	(1.76)	1.08	0.79	0.32	0.20	-0.05
2d <sub>3/2</sub>	2.43	1.70	1.49	0.93	0.60	0.44	-0.11

TABLE IX. Single-quasiparticle binding energies for neutrons in the odd molybdenum isotopes.

State	Mo <sup>93</sup>	Mo <sup>95</sup>	Mo <sup>97</sup>	Mo <sup>99</sup>	Mo <sup>101</sup>
0	8.08	7.36	6.81	5.91	5.39
2d <sub>5/2</sub>	7.95	7.06	6.71	5.81	5.08
3s <sub>1/2</sub>	6.45	5.91	5.83	5.91	5.04
1g <sub>7/2</sub>	5.78	5.30	5.63	5.49	5.13
2d <sub>3/2</sub>	5.65	5.36	5.22	5.18	5.19

estimate of the single-quasiparticle energies:

$$E_j = \frac{\sum_n E_j^{(n)}(2j+1)S_j^{(n)}(d,p) + \sum_m E_j^{(m)}S_j^{(m)}(d,t)}{2j+1} \quad (10)$$

Since, in our case, the difference in  $\sum_n(2j+1)S_j^{(n)}(d,p) + \sum_m S_j^{(m)}(d,t)$  and  $2j+1$  is due more to uncertainties in the experimental data than to a significant departure, we prefer to make the following estimate:

$$E_j = \frac{\sum_n E_j^{(n)}(2j+1)S_j^{(n)}(d,p) + \sum_m E_j^{(m)}S_j^{(m)}(d,t)}{\sum_n (2j+1)S_j^{(n)}(d,p) + \sum_m S_j^{(m)}(d,t)} \quad (11)$$

Values of  $E_j - E_{5/2}$  could be obtained in this way for Mo<sup>100</sup> and Mo<sup>98</sup>, where the  $(d,t)$  data are good and the result is listed in Table VIII. In the calculations it was assumed that  $E_j^{(g.s.)}$  could be taken as the odd-even mass difference. From Table VIII we note that the single-quasiparticle energies obtained in this fashion generally fall nicely between those of the neighboring odd nuclei. From the measured  $Q$  values of  $(d,p)$  and  $(d,t)$  reactions on the molybdenum isotopes,<sup>22</sup> we also computed the single-quasiparticle binding energies. They are listed in Table IX.

### C. Occupancy Numbers

From Table VII and (2) and (3), neglecting the  $\varphi$ 's, we can obtain  $U_j^2$  and  $V_j^2$ . The values obtained in this way do, in general, not fulfill (4) and

$$\sum (2j+1)V_j^2 = \text{number of neutrons present.} \quad (7')$$

$V_j^2$  was therefore determined as

$$V_j^2 = \frac{S_j(d,t)}{(2j+1)S_j(d,p) + S_j(d,t)} \quad (12)$$

to ensure (4), and after that an over-all normalization was made so that (7') was satisfied. In all cases  $\sum V_j^2(2j+1)$  originally turned out to be too large by 30%, indicating an error in the normalization of  $S(d,t)$ . The results obtained in this way are listed in Table X. The accuracy of the results is limited by

<sup>22</sup> B. L. Cohen, R. Patell, A. Prakash, and E. J. Schneid, Phys. Rev. 135, B383 (1964).

uncertainties in the spectroscopic factors particularly  $S(d,t)$  to about 30% except for Mo<sup>100</sup>, where uncertainties in the assignment may introduce errors in excess of that. For Mo<sup>96</sup> and Mo<sup>98</sup>, the reactions Mo<sup>95</sup> $(d,p)$ Mo<sup>96</sup> g.s. and Mo<sup>97</sup> $(d,p)$ Mo<sup>98</sup> g.s. gives an additional check on  $V_{5/2}^2$ . Since almost all the strength goes into the ground state for these reactions, we have according to Yoshida<sup>5</sup>

$$V_{5/2}^2 \approx S_{5/2} / (2 \cdot \frac{5}{2} + 1), \quad (13)$$

where  $V_{5/2}^2$  refers to the even-even nucleus. The values obtained, if the normalizing condition (4) is imposed, are in good agreement with those obtained from  $(d,p)$  and  $(d,t)$  reactions on even-even target nuclei as can be seen in Table X.

TABLE X. Occupancy numbers  $V_j^2$  for the even-even molybdenum isotopes as obtained from  $(d,p)$  and  $(d,t)$  reactions.

State	Mo <sup>92</sup>	Mo <sup>94</sup>	Mo <sup>96</sup>	Mo <sup>96</sup> a	Mo <sup>98</sup>	Mo <sup>98</sup> a	Mo <sup>100</sup>
2d <sub>5/2</sub>	...	0.29	0.50	0.48	0.56	0.64	0.50
3s <sub>1/2</sub>	...	...	0.19	...	0.29	...	0.15
1g <sub>7/2</sub>	...	...	...	...	0.17	...	0.34
2d <sub>3/2</sub>	...	...	0.05	...	0.16	...	0.50

a Obtained from  $(d,p)$  reactions only.

### V. DISCUSSION

The relative single-particle energies for molybdenum,  $\epsilon_j - \epsilon_{5/2}$ , should be equal to the relative single-quasiparticle energies for Mo<sup>93</sup> because Mo<sup>92</sup> forms a closed neutron shell. These energies are displayed in Fig. 7, together with corresponding energies for neighboring even  $Z$  elements. The single-particle energies for molybdenum fits in rather smoothly between those for zirconium and palladium. In zirconium, the  $2p_{1/2}$  proton shell is just filled, and when two more protons are added to make molybdenum they go into the  $1g_{9/2}$  shell. The  $2p_{1/2}$  and the  $1g_{9/2}$  single-particle levels are rather close, so in practice a considerable configuration mixing occurs, e.g., the ground-state wave function of Zr<sup>90</sup> is estimated to be  $(0.75)^{1/2}(2p_{1/2})_0^2 + (0.25)^{1/2}(1g_{9/2})_0^2$ .<sup>7</sup> Due to the presence of the two  $g_{9/2}$  protons, the  $1g_{7/2}$  neutron state is expected to move down due to the long-range neutron-proton interaction. Although we have only observed 37% of the  $1g_{7/2}$  strength so the  $1g_{7/2}$  single-particle level is rather poorly determined, it seems indeed as if the  $1g_{7/2}$  level has moved down somewhat between zirconium and molybdenum. The same is also true but to a less extent for the  $2d_{3/2}$  level.

If the main effect of the interaction between neutrons and protons is absorbed by the single-particle energies as is suggested by the theory of Bremond and Valatin,<sup>23</sup> then the  $(d,p)$  spectra of the molybdenum and the zirconium isotopes should be rather similar because

<sup>23</sup> B. Bremond and J. G. Valatin, Nucl. Phys. 41, 640 (1963).

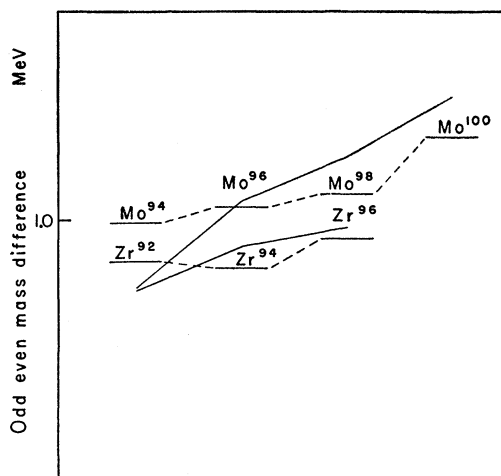


FIG. 8. The fit of the pairing theory calculation to the odd-even mass difference in Zr and Mo. The horizontal lines connected with dashed lines are the experimentally obtained differences. The upper and lower solid lines are the results of pairing theory calculations on molybdenum, with  $G=0.33$ , and on zirconium with  $G=0.30$ , respectively.

their single-particle energies are almost the same. This is certainly the case for  $\text{Mo}^{92}(d,p)\text{Mo}^{93}-\text{Mo}^{96}(d,p)\text{Mo}^{97}$  and  $\text{Zr}^{90}(d,p)\text{Zr}^{91}-\text{Zr}^{94}(d,p)\text{Zr}^{95}$  as can be seen from Fig. 6. However, when we compare  $\text{Mo}^{98}(d,p)\text{Mo}^{99}$  with  $\text{Zr}^{96}(d,p)\text{Zr}^{97}$ , the difference is tremendous. In  $\text{Zr}^{96}(d,p)\text{Zr}^{97}$  the first excited state is at 1.1 MeV and no  $d_{5/2}$  transition could be found below 1.4 MeV. In  $\text{Mo}^{98}(d,p)\text{Mo}^{99}$  there is a strong  $d_{5/2}$  transition to a level only 0.100 MeV above the ground state, and there are 9 more strongly excited states below 0.9 MeV.  $\text{Zr}^{96}$  behaves like a closed-shell nucleus. It is  $\sim 100\%$  full in  $2d_{5/2}$ , the energy of its collective  $2^+$  state is very high (1.7 MeV versus 0.9 MeV in  $\text{Zr}^{92}$  and  $\text{Zr}^{94}$ ), and there is a discontinuity of 0.6 MeV in the ground-state masses.  $\text{Mo}^{98}$ , on the other hand, is only 60% full in  $2d_{5/2}$ , its collective  $2^+$  state is at the same excitation as

in  $\text{Mo}^{94}$  and  $\text{Mo}^{96}$ , and there is essentially no discontinuity in the ground-state masses. To explain this difference we obviously need a theory of neutron-proton interaction. A satisfactory theory on that subject is not available. Therefore, we have tried to fit the data with a simple pairing-force calculation to see how well this theory described experiment and in the hope that deviations from the calculations may shed some light on the neutron-proton interaction problem. The calculations were performed with the help of a code written by Kuo, which not only solved the basic equations of the pairing theory, but it also corrected the single-particle energies for self-binding by the method given by Baranger.<sup>4</sup> The code was tailored for the tin region, and it also incorporated the  $h_{11/2}$  state on which no experimental information had been obtained. In zirconium, the  $h_{11/2}$  state is believed to lie more than 5 MeV above the ground state, and for our calculations it was assumed that the  $h_{11/2}$  state was at 5 MeV. Since the state lies so high, the calculations are fairly insensitive to the exact position of this level. The  $\epsilon_j$ 's were taken as the single-quasiparticle energies in  $\text{Mo}^{93}$  and  $\text{Zr}^{91}$ , and the strength of the pairing interaction  $G$  was chosen in both cases so that the odd-even mass difference was reasonably described (Fig. 8). No attempt was made to change  $G$  with mass number. The odd-even mass difference was obtained from the neutron separation energies (S.E.) according to the formula

$$P = \frac{1}{4}[2 \text{ S.E.}(N) - \text{S.E.}(N-1) - \text{S.E.}(N+1)]. \quad (14)$$

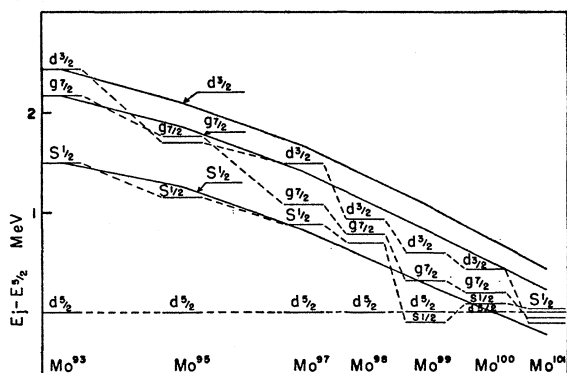
The theoretical binding energies for even-even nuclei were taken as minus the vacuum energies which were calculated by the code as

$$E_{\text{vac}} = \sum_j (2j+1) V_j^2 (\epsilon_j - \lambda - \mu_j/2) - \Delta^2/G, \quad (15)$$

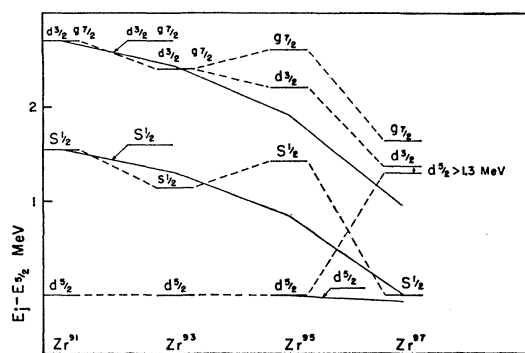
$\lambda$  = Fermi level,

$\mu_j$  = parameter of self-binding,<sup>4</sup>

$\Delta$  = energy gap.<sup>1-3</sup>



(a)



(b)

FIG. 9. Single-quasiparticle energies relative to the  $\frac{5}{2}^+$  single-quasiparticle energy in  $\text{Mo}^{93}-\text{Mo}^{101}$  and  $\text{Zr}^{91}-\text{Zr}^{97}$ . The experimentally measured energies are the horizontal lines connected by dashed lines. The solid lines are the result of pairing-theory calculations with parameters as described in the text.

The binding energies (B.E.) for the even-odd nuclei were obtained from

$$\text{B.E.}(N+1) = \text{B.E.}(N) - \lambda - [(\epsilon_j - \lambda - \mu_j/2)^2 + \Delta^2]^{1/2}. \quad (16)$$

The experimental and predicted single-quasiparticle energies for the molybdenum and zirconium isotopes are shown in Fig. 9 and the experimental and predicted occupancy numbers in Fig. 10. From Figs. 9 and 10 we observe:

(1) The fit for the relative single-quasiparticle energies in zirconium is not good, e.g., the calculations completely fails to account for the position of the  $d_{5/2}$  state in  $\text{Zr}^{97}$ .

(2) For molybdenum the experimental single-quasiparticle energies for the  $g_{7/2}$  and  $d_{3/2}$  levels tend to be lower than the calculated for  $\text{Mo}^{97}$ — $\text{Mo}^{101}$ .

(3) The experimental occupancy numbers in molybdenum for the  $s_{1/2}$ ,  $g_{7/2}$ , and  $d_{3/2}$  states are much larger, and for the  $d_{5/2}$  state, smaller than the calculated.

(4) The pairing interaction  $G$  seems to be stronger in molybdenum than in zirconium 0.33 versus 0.30.

It may be worth noting that in zirconium we could have obtained a better fit to the relative quasiparticle energies at the sacrifice of the fit to the odd-even mass difference by making  $G$  smaller. In molybdenum a slightly smaller  $G$  and a smaller value of  $\epsilon_{7/2} - \epsilon_{5/2}$  and  $\epsilon_{3/2} - \epsilon_{5/2}$  would have given a better over-all fit to the experimental data. We also note that the experimental values of  $V_j^2$  are subject to rather large errors, so the discrepancy is not necessarily a deficiency of the theory only. That the strength of the pairing interaction  $G$  comes out larger in molybdenum than in zirconium is not in accord with the idea of a  $G$  varying smoothly from isotope to isotope. However, in determining  $G$  from the odd-even mass difference, we assumed that the position of the  $h_{11/2}$  (and other higher levels) did not change between molybdenum and zirconium. Since the expression for  $\Delta$ , which is essentially the odd-even mass difference, is a sum over levels which it does not even converge, the change in the odd-even mass difference between molybdenum and zirconium need not necessarily mean a change in  $G$ .

From the above remarks we conclude that, apart from the occupancy numbers, molybdenum is qualitatively described by simple pairing theory, whereas the

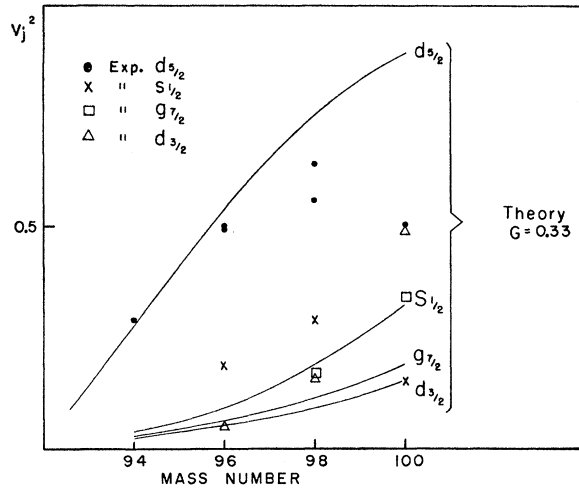


FIG. 10. A comparison between the experimentally measured occupancy numbers  $V_j^2$  and those obtained from the calculations which were used to fit the energies. The curves connect the numbers obtained from the calculation; the various points are from the experiment.

description of zirconium is not so good. It is true that a better fit to the single-quasiparticle energies may have been obtained if a more refined theory taking the three-quasiparticle excitation into account had been employed. However, it is hard to believe that any theory taking only neutrons into account can produce great changes in zirconium and not in molybdenum. We thus conclude that the different behavior of the single-quasiparticle energies in molybdenum and zirconium cannot be explained accurately by a pure neutron theory and absorbing the neutron-proton interaction in the single-particle energies.

#### ACKNOWLEDGMENTS

The authors would like to express their extreme gratitude to T. S. Kuo, who make his code available to us prior to publishing his own calculations, and to E. K. Lin, who arranged the calculations on the University of Pittsburgh's IBM 7090. The authors would also like to thank Dr. R. M. Drisko for helpful discussions and for carrying out the DWBA calculations, Dr. E. Baranger for many helpful discussions, the cyclotron operations group, and the plate reading group under the direction of Mrs. A. Trent.